Rapamycin-Induced Insulin Resistance Is Mediated by mTORC2 Loss and Uncoupled from Longevity

Dudley W. Lamming *et al.*

Science **335**, 1638 (2012);
DOI: 10.1126/science.1215135

Science (print ISSN 0036-8075; online ISSN 1095-9203) is published weekly, except the last week in December, by the American Association for the Advancement of Science, 1200 New York Avenue NW, Washington, DC 20005.

link function (Proc Genmod, SAS 9.1, SAS Institute Incorporated, Cary, North Carolina). When the infection assays were run over two time blocks, the model also included a block effect and a time-by-block interaction.

The infection assays showed a significant evolutionary response of hosts to epidemics in six of seven lake populations. In three lakes (Island, Midland, and Scott Lakes), host populations became significantly more resistant during epidemics (Fig. 1). However, in three other populations (Canvasback, Downing, and Hale Lakes), hosts became significantly more susceptible to infection. The hosts in the seventh lake, Beaver Dam, did not show a significant change in susceptibility but trended toward increased resistance.

As anticipated by theory (SOM), these evolutionary trajectories correlated with ecologically driven variation in epidemic size. Among the six lake populations showing a significant evolutionary response, change in mean susceptibility correlated strongly with epidemic size (Pearson correlation: $r = 0.86$, $P = 0.030$, $n = 6$; Fig. 2A). Further, in those six lakes, epidemics were larger at lower predation intensity (larger size of hosts; Pearson correlation: $r = 0.86$, $P = 0.029$, $n = 6$; Fig. 2B) and where total nitrogen was higher (Pearson correlation: $r = 0.83$, $P = 0.040$, $n = 6$; Fig. 2C); the trend was similarly directed, but not significant, for total phosphorus (Pearson correlation: $r = 0.50$, $P = 0.3$, $n = 6$; Fig. 2D). Overall, hosts became more susceptible to the yeast in lower productivity lakes with higher vertebrate predation but evolved toward decreased susceptibility in more productive lakes with lower vertebrate predation (Fig. 2, E and F; t tests for differences between two groups; results for body size, $t_4 = 3.19$ and $P = 0.033$; nitrogen, $t_4 = 3.18$ and $P = 0.034$; phosphorus, $t_4 = 0.88$ and $P = 0.43$). Thus, ecological gradients, through their effects on epidemic size, influenced evolutionary outcomes of hosts during outbreaks of a virulent parasite. These qualitative predictions also arose from a general, trait-based epidemiological model built for similar epidemiology and parameterized for our particular system (SOM).

These results show that hosts can evolve enhanced susceptibility to their virulent parasites during epidemics [also see (*27*) for a similar but unreplicated occurrence]. A combination of observations, experiments, and modeling all suggest causation for this initially counterintuitive finding. When ecological factors promote large epidemics, hosts should evolve to become more resistant to infection. However, resistance-fecundity trade-offs can prompt host populations to evolve increased susceptibility when ecology constrains epidemic size. Overall, we demonstrated that ecological context influences epidemic size, which, in turn, determines evolutionary responses of hosts to epidemics. This suggests that alteration of predation pressure on hosts and productivity of ecosystems may influence the ecology and evolution of host-parasite interactions.

References and Notes

1. M. A. Duffy, S. E. Forde, *J. Anim. Ecol.* **78**, 1106 (2009).
2. R. M. Penczykowski, S. E. Forde, M. A. Duffy, *Freshw. Biol.* **56**, 689 (2011).
3. M. F. Dybdahl, C. M. Lively, *Evolution* **52**, 1057 (1998).
4. J. Jokela, M. F. Dybdahl, C. M. Lively, *Am. Nat.* **174** (suppl. 1), S43 (2009).
5. J. Antonovics, P. H. Thrall, *Proc. Biol. Sci.* **257**, 105 (1994).
6. M. Boots, A. Best, M. R. Miller, A. White, *Philos. Trans. R. Soc. London Ser. B* **364**, 27 (2009).
7. M. Boots, Y. Haraguchi, *Am. Nat.* **153**, 359 (1999).
8. R. G. Bowers, M. Boots, M. Begon, *Proc. Biol. Sci.* **257**, 247 (1994).
9. R. M. Anderson, R. M. May, *Infectious Diseases of Humans: Dynamics and Control* (Oxford Univ. Press, Oxford, 1991).
10. M. J. Keeling, P. Rohani, *Modeling Infectious Diseases in Humans and Animals* (Princeton Univ. Press, Princeton, NJ, 2008).
11. K. D. Lafferty, R. D. Holt, *Ecol. Lett.* **6**, 654 (2003).
12. C. Packer, R. D. Holt, P. J. Hudson, K. D. Lafferty, A. P. Dobson, *Ecol. Lett.* **6**, 797 (2003).
13. S. R. Hall, C. R. Becker, M. A. Duffy, C. E. Cáceres, *Am. Nat.* **176**, 557 (2010).
14. M. A. Duffy, L. Sivars-Becker, *Ecol. Lett.* **10**, 44 (2007).
15. M. A. Duffy, S. R. Hall, *Am. Nat.* **171**, 499 (2008).
16. S. R. Hall, C. R. Becker, M. A. Duffy, C. E. Cáceres, *Oecologia* **166**, 833 (2011).
17. E. P. Overholt *et al.*, *Ecol. Lett.* **15**, 47 (2012).
18. M. A. Duffy *et al.*, *BMC Evol. Biol.* **8**, 80 (2008).
19. M. A. Duffy, S. R. Hall, C. E. Cáceres, A. R. Ives, *Ecology* **90**, 1441 (2009).
20. S. R. Hall *et al.*, *Bioscience* **60**, 363 (2010).
21. M. A. Duffy, S. R. Hall, A. J. Tessier, M. Huebner, *Limnol. Oceanogr.* **50**, 412 (2005).
22. A. E. Greenberg *et al.*, Eds., *Standard Methods for the Examination of Water and Wastewater* (American Public Health Association, Washington, DC, ed. 19, 1995).
23. J. J. Elser *et al.*, *Ecol. Lett.* **10**, 1135 (2007).
24. S. J. Guildford, R. E. Hecky, *Limnol. Oceanogr.* **45**, 1213 (2000).
25. J. L. Brooks, S. I. Dodson, *Science* **150**, 28 (1965).
26. J. A. Kitchell, J. F. Kitchell, *Limnol. Oceanogr.* **25**, 389 (1980).
27. M. A. Parker, *Evolution* **45**, 1209 (1991).

Acknowledgments: We thank S. Hernandez, K. Jansen, K. Kenline, A. Reynolds, B. Sarrell, K. van Rensburg, and C. Washington for assistance in the lab; K. Boatman, Z. Brown, A. Bowling, C. White, and P. Forys for their help with the field survey; and S. Auld and two anonymous reviewers for comments on the manuscript. This work was supported by NSF (grants DEB-0841679 to M.A.D., DEB-0841817 to S.R.H., and DEB-0845825 and OCE-0928819 to C.A.K.) and by a grant from the James S. McDonnell Foundation (to C.A.K.). We appreciate cooperation from S. Siscoe at the Indiana Department of Natural Resources's Division of Forestry and R. Ronk at the Division of Fish and Wildlife for the field survey. This is KBS contribution no. 1607. Data are available in the SOM and from the lead author (M.A.D.).

Supporting Online Material

www.sciencemag.org/cgi/content/full/335/6076/1636/DC1
Materials and Methods
Fig. S1
Tables S1 and S2
References (*28*–*32*)

18 October 2011; accepted 28 February 2012
10.1126/science.1215429

Rapamycin-Induced Insulin Resistance Is Mediated by mTORC2 Loss and Uncoupled from Longevity

Dudley W. Lamming,[1,2,3,4,5]† Lan Ye,[6]† Pekka Katajisto,[1,2,3,4,5] Marcus D. Goncalves,[7] Maki Saitoh,[1,2,3,4,5] Deanna M. Stevens,[1,2,3,4,5] James G. Davis,[6] Adam B. Salmon,[8] Arlan Richardson,[8] Rexford S. Ahima,[7] David A. Guertin,[1,2,3,4,5]* David M. Sabatini,[1,2,3,4,5]‡ Joseph A. Baur[6]‡

Rapamycin, an inhibitor of mechanistic target of rapamycin complex 1 (mTORC1), extends the life spans of yeast, flies, and mice. Calorie restriction, which increases life span and insulin sensitivity, is proposed to function by inhibition of mTORC1, yet paradoxically, chronic administration of rapamycin substantially impairs glucose tolerance and insulin action. We demonstrate that rapamycin disrupted a second mTOR complex, mTORC2, in vivo and that mTORC2 was required for the insulin-mediated suppression of hepatic gluconeogenesis. Further, decreased mTORC1 signaling was sufficient to extend life span independently from changes in glucose homeostasis, as female mice heterozygous for both mTOR and mLST8 exhibited decreased mTORC1 activity and extended life span but had normal glucose tolerance and insulin sensitivity. Thus, mTORC2 disruption is an important mediator of the effects of rapamycin in vivo.

Age-related diseases—including cancer, neurodegenerative disorders, cardiovascular disease, type II diabetes, and many others—are the major contributors to morbidity and mortality in Western society. The high frequency of these diseases in the elderly limits the benefit that can be obtained by targeting them individually (*1*). However, targeting the aging process directly may offer a way to delay the incidence of many age-related diseases simultaneously. To date, the only molecule that appears to influence the intrinsic rate of aging in mammals, as evidenced by a robust extension of maximum life span, is rapamycin, an inhibitor of mechanistic (previously referred to as mammalian) target of rapamycin complex 1 (mTORC1) (*2*, *3*).

mTOR is a kinase that integrates inputs from many nutrients and growth factors. mTOR is found in two distinct protein complexes: mTORC1, which regulates numerous cellular processes related to

growth and differentiation, and mTORC2, which has a regulatory role in the insulin signaling cascade. Genetic attenuation of mTORC1 signaling promotes longevity in diverse organisms, including *Saccharomyces cerevisiae*, *Caenorhabditis elegans*, and *Drosophila melanogaster*, and rapamycin-induced life span extension has been reported in *S. cerevisiae*, *D. melanogaster*, and mice (*2*–*7*). Moreover, deletion of the mTORC1 substrate S6 kinase 1 (S6K1) is sufficient to confer increased life-span in female mice (*8*). These findings strongly implicate mTOR in the regulation of mammalian longevity.

Calorie restriction (CR), a reduction in caloric intake while maintaining adequate nutrition, improves health and extends life-span in many organisms, including primates, through a mechanism that is not understood (*9*, *10*). Yeast that lack the mTOR homolog *TOR1* have an extended replicative life span that is not further enhanced by CR, which suggests a common mechanism (*4*), but in flies, rapamycin increases life span beyond the maximum achieved by CR and thus may act through additional mechanisms (*11*). Improved glucose tolerance and insulin sensitivity are hallmarks of CR in mammals and a common feature of many models of increased longevity (*12*–*16*), although mice lacking insulin receptor substrate (IRS) proteins 1 or 2 provide a notable counterexample (*17*, *18*). One possible mechanism for enhanced insulin sensitivity during CR is reduced negative feedback through a signaling loop mediated by mTORC1 and S6K1 (*19*). Indeed, deletion of S6K1 is sufficient to improve insulin sensitivity and to extend life in mice (*8*), which suggests that rapamycin might act in a similar manner.

In contrast to the prediction that rapamycin would mimic the effects of CR or S6K1 deletion on glucose tolerance and insulin sensitivity, recent evidence suggests that chronic treatment with rapamycin impairs glucose homeostasis. Prolonged treatment with rapamycin leads to glucose intolerance in mice (*20*), as well as insulin resistance in rats (*21*, *22*) and possibly humans (*23*, *24*). We explored the mechanism by which rapamycin treatment impairs glucose homeostasis. Chronic rapamycin treatment, at approximately the same dose that was used to extend life span (~2 mg/kg per day), led to glucose intolerance and insulin resistance in both male and

[1]Whitehead Institute for Biomedical Research, Cambridge, MA 02142, USA. [2]Department of Biology, Massachusetts Institute of Technology (MIT), Cambridge, MA 02139, USA. [3]Howard Hughes Medical Institute, MIT, Cambridge, MA 02139, USA. [4]Broad Institute of Harvard and MIT, Seven Cambridge Center, Cambridge, MA 02142, USA. [5]The David H. Koch Institute for Integrative Cancer Research at MIT, Cambridge, MA 02139, USA. [6]Department of Physiology, Institute for Diabetes, Obesity, and Metabolism, Perelman School of Medicine, University of Pennsylvania, Philadelphia, PA 19104, USA. [7]Department of Medicine, Institute for Diabetes, Obesity, and Metabolism, Perelman School of Medicine, University of Pennsylvania, Philadelphia, PA 19104, USA. [8]The Barshop Institute for Longevity and Aging Studies, University of Texas Health Science Center at San Antonio, San Antonio, TX 78245, USA.

*Present address: University of Massachusetts Medical School, Worcester, MA 01655, USA.

†These authors contributed equally to this work

‡To whom correspondence should be addressed. E-mail: baur@mail.med.upenn.edu (J.A.B.); sabatini@wi.mit.edu (D.M.S.)

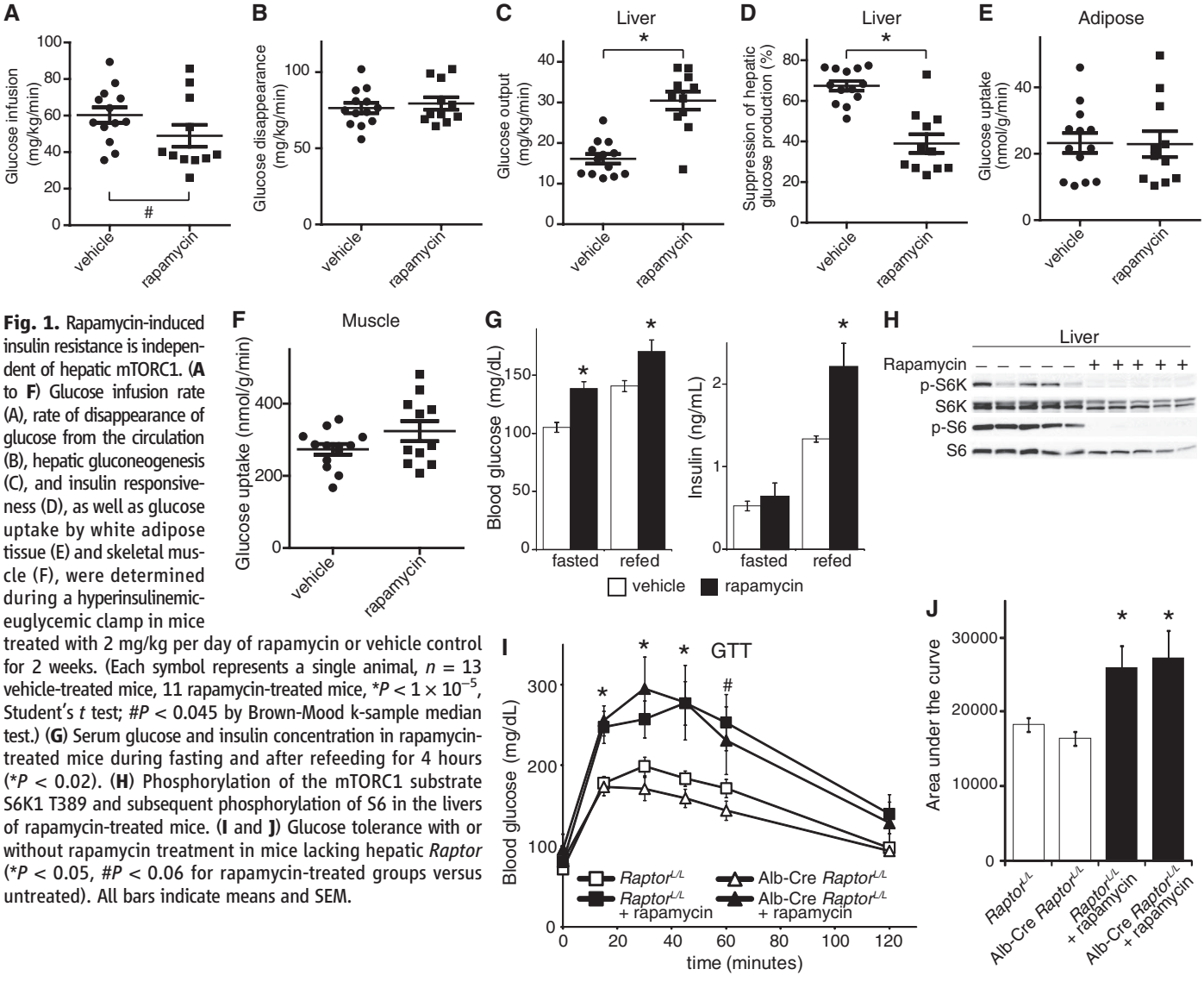

Fig. 1. Rapamycin-induced insulin resistance is independent of hepatic mTORC1. (**A** to **F**) Glucose infusion rate (A), rate of disappearance of glucose from the circulation (B), hepatic gluconeogenesis (C), and insulin responsiveness (D), as well as glucose uptake by white adipose tissue (E) and skeletal muscle (F), were determined during a hyperinsulinemic-euglycemic clamp in mice treated with 2 mg/kg per day of rapamycin or vehicle control for 2 weeks. (Each symbol represents a single animal, $n = 13$ vehicle-treated mice, 11 rapamycin-treated mice, $^*P < 1 \times 10^{-5}$, Student's t test; $\#P < 0.045$ by Brown-Mood k-sample median test.) (**G**) Serum glucose and insulin concentration in rapamycin-treated mice during fasting and after refeeding for 4 hours ($^*P < 0.02$). (**H**) Phosphorylation of the mTORC1 substrate S6K1 T389 and subsequent phosphorylation of S6 in the livers of rapamycin-treated mice. (**I** and **J**) Glucose tolerance with or without rapamycin treatment in mice lacking hepatic *Raptor* ($^*P < 0.05$, $\#P < 0.06$ for rapamycin-treated groups versus untreated). All bars indicate means and SEM.

female C57BL/6 mice (fig. S1, A and B). In rats, rapamycin-induced glucose intolerance results, in part, from increased hepatic gluconeogenesis (*22*). We found that rapamycin-treated mice had increased expression of the gluconeogenic genes for phosphoenolpyruvate carboxykinase (PEPCK) and glucose 6-phosphatase (G6Pase) in their livers and had substantially impaired tolerance to pyruvate, which indicated a failure to suppress gluconeogenesis (fig. S1, C and D).

We used a hyperinsulinemic-euglycemic clamp to measure insulin sensitivity in rapamycin-treated

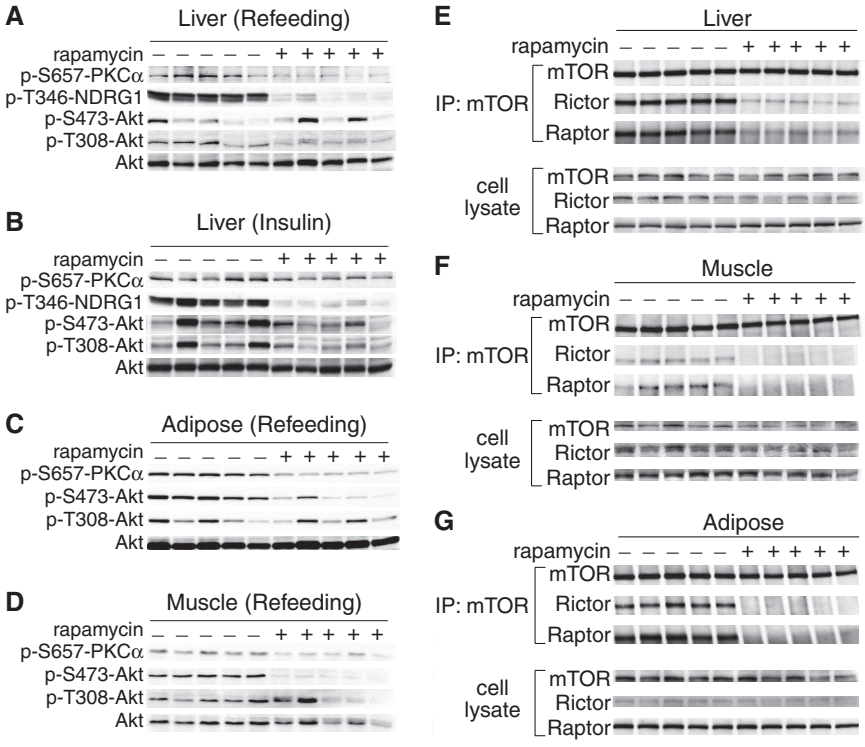

Fig. 2. Disruption of mTORC2 in vivo after chronic rapamycin treatment. (**A** and **B**) Effects of rapamycin on phosphorylation of PKCα, Akt, and the SGK substrate NDRG1 in liver in response to refeeding (A) or insulin (B) after an overnight fast. (**C** and **D**) Effects of rapamycin on phosphorylation of PKCα and Akt in response to refeeding in white adipose tissue (C) and muscle (D). (**E** to **G**) Effects of rapamycin on the integrity of mTORC1 and mTORC2. mTOR was immunoprecipitated from liver (E), skeletal muscle (F), and white adipose tissue (G), followed by immunoblotting for Raptor and Rictor (subunits of mTORC1 and mTORC2, respectively).

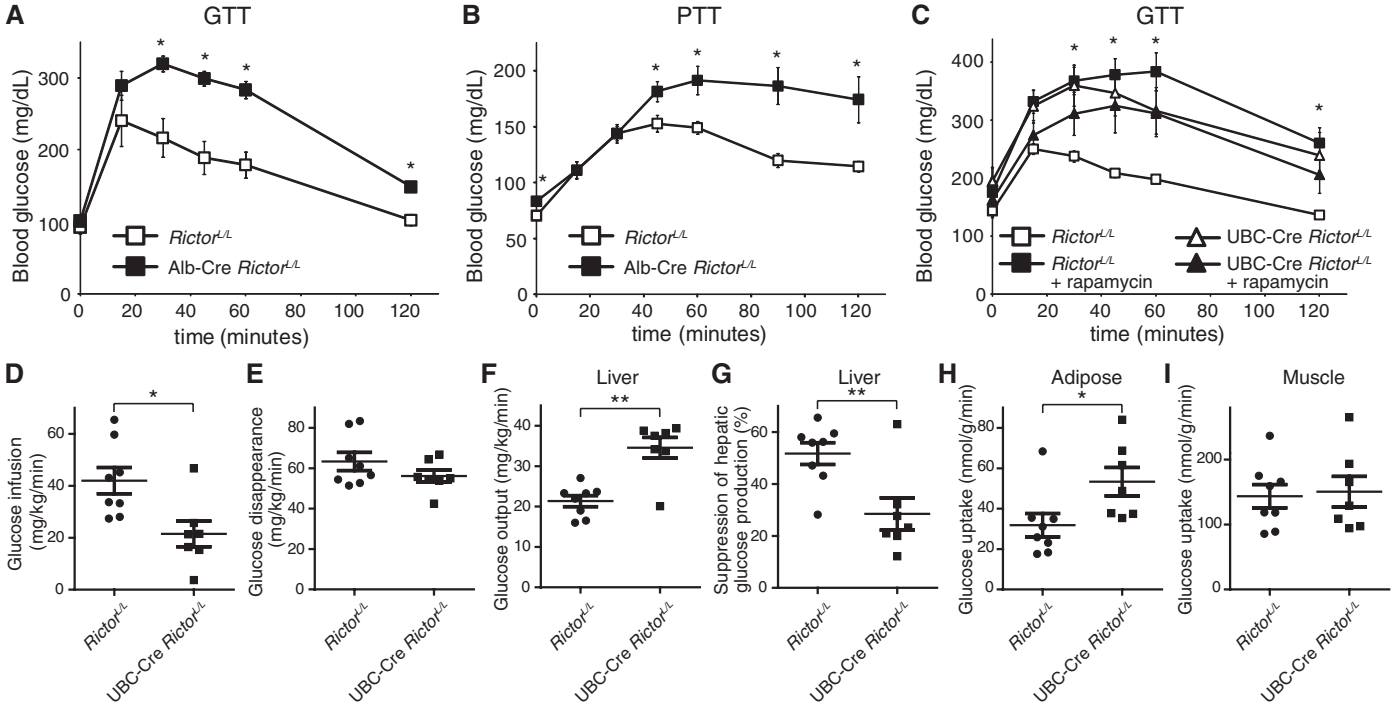

Fig. 3. Regulation of glucose homeostasis by mTORC2. (**A**) Glucose tolerance of Alb-Cre *Rictor*$^{LoxP/LoxP}$ mice (*$P < 0.002$). (**B**) Pyruvate tolerance of Alb-Cre *Rictor*$^{loxP/loxP}$ mice (*$P < 0.03$). (**C**) Effect of rapamycin on glucose tolerance of mice with whole-body deletion of Rictor fasted for 6 hours (*$P < 0.008$ for all groups versus *Rictor*$^{loxP/loxP}$). (**D** to **I**) Glucose infusion rate (D), rate of disappearance of glucose from the circulation (E), hepatic gluconeogenesis (F), and insulin responsiveness (G), as well as glucose uptake by white adipose tissue (H) and skeletal muscle (I), were determined during a hyperinsulinemic-euglycemic clamp in tamoxifen-treated ubiquitinC–CreERT2 *Rictor*$^{loxP/loxP}$ mice fasted for 6 hours ($n = 8$ *Rictor*$^{loxP/loxP}$, 7 UBC-Cre *Rictor*$^{loxP/loxP}$, **$P < 0.008$; *$P < 0.05$). All bars indicate means and SEM.

mice (Fig. 1, A to F). Briefly, mice received a constant infusion of insulin, and radiolabeled glucose was coinfused as needed to prevent hypoglycemia. Calculating whole-body glucose uptake and hepatic glucose production, based on the fraction of labeled glucose in the circulation, revealed marked hepatic insulin resistance in rapamycin-treated mice (Fig. 1, C and D). In contrast, uptake of labeled glucose into white adipose and skeletal muscle was unaffected under clamp conditions (Fig. 1, E and F). In rapamycin-treated animals, plasma insulin was unchanged during fasting and higher after refeeding (Fig. 1G), which suggested an adaptive response to insulin resistance rather than a defect in insulin production by pancreatic beta cells. These results indicate that hepatic insulin resistance is a major contributor to the impairment of glucose homeostasis by rapamycin and that white adipose tissue and skeletal muscle take up glucose normally in response to continuous insulin stimulation, despite inhibition of mTORC1 signaling to S6K1 in all three tissues (Fig. 1H and fig. S2, A and B).

We specifically disrupted hepatic mTORC1 signaling by expressing Cre under the control of the liver-specific albumin promoter in mice carrying a conditional allele of the mTORC1 subunit Raptor (regulatory associated protein of mTOR) (fig. S2C). Alb-Cre *Raptor*$^{loxP/loxP}$ mice, despite lacking hepatic mTORC1 activity, had normal glucose tolerance and remained responsive to rapamycin treatment (Fig. 1, I and J). These results indicate that disruption of hepatic mTORC1 signaling cannot account for the effects of rapamycin on glucose homeostasis. Although rapamycin is generally considered to be a specific inhibitor of mTORC1, extended treatment of cells with rapamycin can also physically disrupt mTORC2, independently from changes in protein expression in certain cell lines (*25*). We therefore examined mTORC2 signaling in livers, white adipose tissue, and muscles from rapamycin-treated

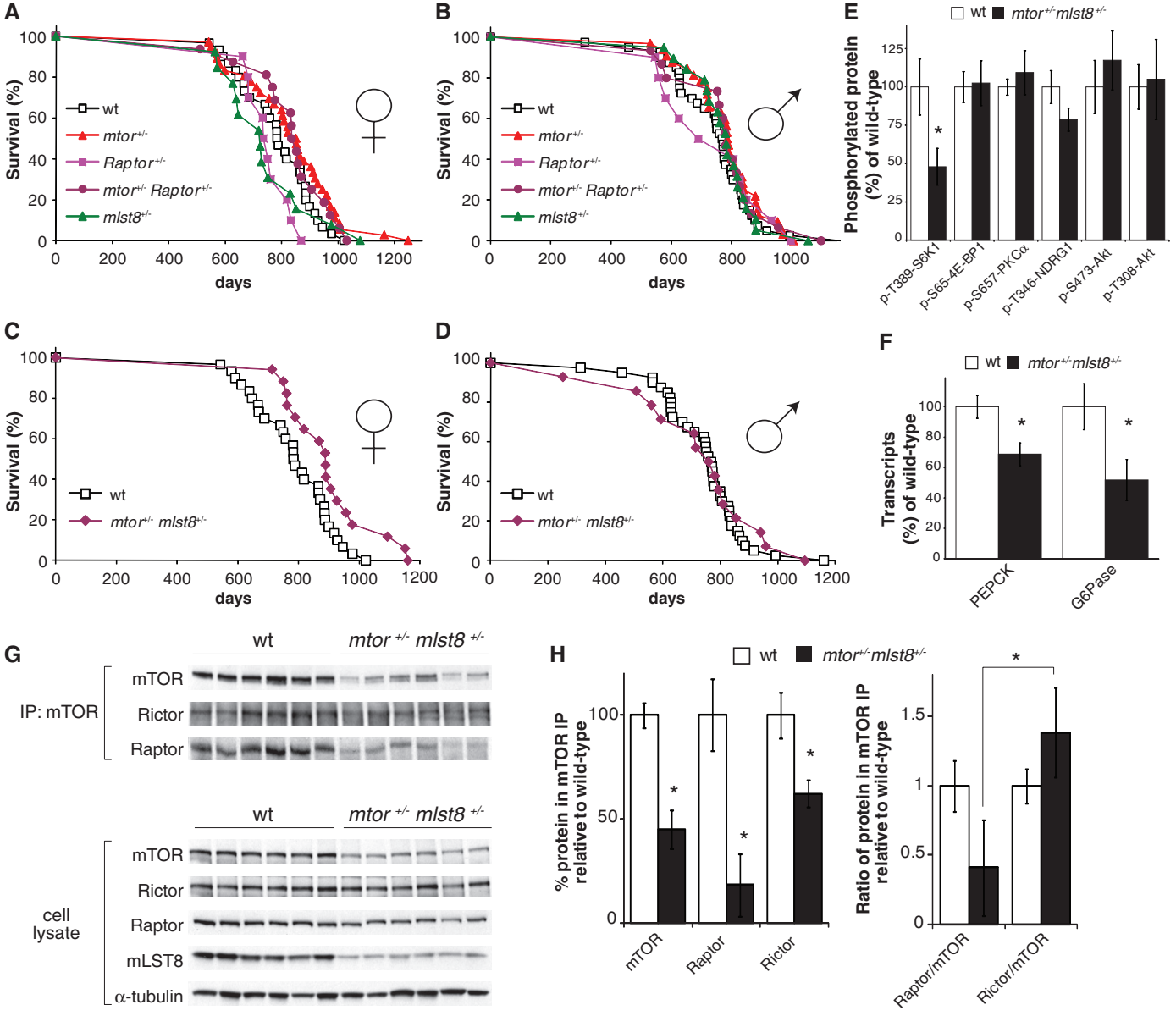

Fig. 4. Depletion of mTOR and mLST8 uncouples longevity from decreased glucose tolerance. (**A** and **B**) Kaplan-Meier plots showing life spans of female (A) and male (B) mice heterozygous for components of the mTOR signaling pathway. (**C** and **D**) Life-spans of female (C) and male (D) *mtor*$^{+/-}$ *mlst8*$^{+/-}$ mice. Wild-type curves are repeated for comparison. (**E**) Quantification of phosphorylated proteins in female wild-type and *mtor*$^{+/-}$ *mlst8*$^{+/-}$ livers after an overnight fast and 45 min of refeeding ($n = 13$ wild-type versus 13 *mtor*$^{+/-}$ *mlst8*$^{+/-}$ female mice, *$P < 0.03$). (**F**) Quantitative real-time polymerase chain reaction analysis of mRNA levels for PEPCK and G6Pase in the livers of young female wild-type and *mtor*$^{+/-}$ *mlst8*$^{+/-}$ mice (*$P < 0.03$). (**G** and **H**) Immunoprecipitation of mTOR complexes reveals preferential loss of Raptor association in *mtor*$^{+/-}$ *mlst8*$^{+/-}$ female mice (*$P < 0.02$). All bars indicate means and SEM.

mice. Mice were fasted overnight and then stimulated by refeeding or by intraperitoneal injection of insulin. Phosphorylation of mTORC2 substrates, including the protein kinases PKCα S657 and Akt S473, as well as the serum glucocorticoid–induced protein kinase (SGK) substrate (N-Myc downstream regulated 1) NDRG1 T346 (Fig. 2, A to D) was attenuated in all three tissues. To confirm that these effects resulted from mTORC2 disruption, we immunoprecipitated mTOR from the liver, white adipose tissue, and skeletal muscle of mice treated with rapamycin, and we visualized components of mTORC1 and mTORC2 by protein immunoblotting (Fig. 2, E to G). Chronic rapamycin treatment disrupted the association of mTOR with both Raptor (mTORC1) and Rictor (Raptor-independent companion of mTOR, mTORC2) in all three tissues. Therefore, direct disruption of mTORC2 is a second molecular mechanism that may contribute to the effects of rapamycin in vivo. Although rapamycin inhibited the phosphorylation of hepatic PKCα and the activity of SGK [as evidenced by decreased phosphorylation of the SGK substrate NDRG1 (*26*)] in animals that were fasted and refed for 45 min, the phosphorylation of hepatic Akt S473 was inhibited by rapamycin only in animals stimulated with insulin (49.7% of wild-type level, $P = 0.013$) (Fig. 2, A and B) (*25*). This may indicate that a small amount of residual mTORC2 is sufficient for basal, but not maximal, signaling to Akt.

To examine the effect of hepatic mTORC2 on glucose homeostasis, we generated mice that carried a Cre-excisable allele of the mTORC2 subunit *Rictor* and expressed Cre under the control of the albumin promoter (fig. S3A). Alb-Cre *Rictor*$^{loxP/loxP}$ mice displayed pronounced glucose intolerance (Fig. 3A), but had a mild defect in an insulin tolerance test (fig. S3B), which likely reflected normal glucose uptake into skeletal muscle and adipose tissue. As with rapamycin-treated mice, Alb-Cre *Rictor*$^{loxP/loxP}$ mice had impaired ability to suppress hepatic gluconeogenesis in a pyruvate tolerance test (Fig. 3B), had increased hepatic expression of G6Pase (fig. S4A), and did not show any overt defect in insulin secretion (fig. S4B). Thus, disruption of mTORC2 in the liver is sufficient to impair hepatic insulin sensitivity and is likely a major contributor to rapamycin-induced glucose intolerance.

Rapamycin disrupts mTORC2 in multiple tissues (Fig. 2, E to G). Deletion of *Rictor* in muscle impairs phosphorylation of Akt S473, although the effect on glucose homeostasis has not been described (*27*). Deletion of *Rictor* in adipose tissue leads to weight gain, hyperinsulinemia, and insulin resistance, with discordant findings reported as to the net effect on glucose tolerance (*28*, *29*). To better understand the consequences of whole-body mTORC2 disruption, we created a strain of mice in which *Rictor* could be conditionally deleted in adult animals with a tamoxifen-inducible Cre (CreERT2) allele expressed under the control of the ubiquitin C promoter.

Consistent with the idea that rapamycin-induced hepatic insulin resistance is primarily mediated by mTORC2 disruption, there was no further effect on glucose homeostasis when ubiquitin C–CreERT2 *Rictor*$^{loxP/loxP}$ mice were treated for 2 weeks with rapamycin (Fig. 3C). Note that Alb-Cre *Rictor*$^{loxP/loxP}$ mice treated with rapamycin were hyperglycemic after 6 hours of fasting (fig. S6A) or refeeding (fig. S4B). This difference may reflect alterations in metabolism as a result of lifelong deficiency in hepatic Rictor. Nevertheless, rapamycin had no further effect on gluconeogenic gene expression, glucose tolerance, or pyruvate tolerance in Alb-Cre *Rictor*$^{loxP/loxP}$ mice (figs. S4A and S6, B to E).

During a hyperinsulinemic-euglycemic clamp (Fig. 3, D to I), tamoxifen-treated ubiquitin C–CreERT2 *Rictor*$^{loxP/loxP}$ mice had a decreased glucose infusion rate compared with tamoxifen-treated *Rictor*$^{loxP/loxP}$ controls (Fig. 3D). As with the rapamycin-treated mice, the predominant defect in these animals under clamp conditions was hepatic insulin resistance, which resulted in increased glucose production (Fig. 3, F and G). Although the overall rates of glucose removal from the blood and uptake into skeletal muscle were not significantly affected, glucose uptake into white adipose tissue was increased (Fig. 3, H and I). Thus, Rictor appears to have a role in the regulation of glucose homeostasis in white adipose tissue, although chronic rapamycin treatment is not sufficient to elicit this phenotype (Fig. 1E), or the effect is offset by other rapamycin targets, such as mTORC1. Notably, *Rictor* was not completely excised in skeletal muscle, meaning that a role for mTORC2 in this tissue cannot be excluded at present. Thus, both rapamycin treatment and *Rictor* deletion induce clear hepatic insulin resistance, whereas the precise role of mTORC2 in regulating glucose uptake into other tissues remains to be fully defined.

Because the negative effects of rapamycin on glucose tolerance and hepatic insulin sensitivity appear to be mediated by mTORC2 disruption, whereas life-span extension has generally been presumed to result from mTORC1 inhibition, it may be possible to uncouple the beneficial and detrimental effects of mTOR inhibition. We therefore bred mice carrying only a single copy of *mtor*, *Raptor*, or *mlst8* (mammalian lethal with Sec13 protein 8), or double-mutant *mtor*$^{+/-}$ *Raptor*$^{+/-}$ and *mtor*$^{+/-}$ *mlst8*$^{+/-}$ mice and followed them as they aged.

There was no increase in life span in either female (Fig. 4A) or male (Fig. 4B) *mtor*$^{+/-}$, *Raptor*$^{+/-}$, *mlst8*$^{+/-}$ or *mtor*$^{+/-}$ *Raptor*$^{+/-}$ mice (see also table S1). However, female *mtor*$^{+/-}$ *mlst8*$^{+/-}$ mice were long-lived, with a 14.4% increase in mean life span relative to wild type (Fig. 4C) (Dunnett's test, $P = 0.046$; Cox $P = 0.027$) (table S1). The longevity of male *mtor*$^{+/-}$ *mlst8*$^{+/-}$ mice was unaffected (Fig. 4D). Female *mtor*$^{+/-}$ *mlst8*$^{+/-}$ mice were not calorie-restricted through reduced food intake or increased energy expenditure and had normal body weights and levels of activity (fig. S7). Consistent with the phenotypic effects, *mtor*$^{+/-}$ *mlst8*$^{+/-}$ mice exhibited a reduction of about 30 to 60% in the abundance of hepatic mTOR, Raptor, mLST8, and Rictor, whereas the expression of mTOR complex subunits was less affected in *Raptor*$^{+/-}$ and *mtor*$^{+/-}$ *Raptor*$^{+/-}$ heterozygotes (fig. S8).

Consistent with the increased life span of female *mtor*$^{+/-}$ *mlst8*$^{+/-}$ mice, hepatic mTORC1 signaling, as assessed by S6K1 phosphorylation, was decreased by ~50% (fig. S9A and Fig. 4E). Although both mTOR and mLST8 are subunits that are shared between the two mTOR complexes, there was no significant change in mTORC2 signaling as assessed by Akt, PKCα, or NDRG1 phosphorylation. Phosphorylation of 4E-BP1 was not changed in the livers of female *mtor*$^{+/-}$ *mlst8*$^{+/-}$ mice; however, we observed decreased phosphorylation of 4E-BP1 in mouse tail fibroblasts in vitro (fig. S10, A and B), which suggested that both S6K and 4E-BP1 signaling may be affected. Hepatic S6K1 T389 phosphorylation was also lower in male *mtor*$^{+/-}$ *mlst8*$^{+/-}$ mice than in controls ($P < 0.08$) (fig. S10C).

Female *mtor*$^{+/-}$ *mlst8*$^{+/-}$ mice had normal glucose tolerance (fig. S9B), insulin sensitivity (fig. S11A), and fasting insulin levels (fig. S11B), which further indicated that mTORC2 signaling was intact. Moreover, female *mtor*$^{+/-}$ *mlst8*$^{+/-}$ mice had decreased expression of PEPCK and G6Pase, which suggested that control of hepatic glucose production may even have been improved (Fig. 4H). Although absolute amounts of both mTORC1 and mTORC2 decreased in the livers of female *mtor*$^{+/-}$ *mlst8*$^{+/-}$ mice, the ratio of Raptor to mTOR declined more than the ratio of Rictor to mTOR (Fig. 4, I and J). Thus, mTORC2 appears to compete more effectively for a limiting amount of the mTOR catalytic subunit.

Glucose tolerance (area under the curve) was not significantly affected in young animals from any of the strains heterozygous for mTORC1 components, although the glucose tolerance of male *Raptor*$^{+/-}$ mice improved with age (fig. S11, C and D). The increased life span and normal glucose tolerance of female *mtor*$^{+/-}$ *mlst8*$^{+/-}$ mice, and the unchanged life-span despite increased glucose tolerance in male *Raptor*$^{+/-}$ mice are both indicative that the effects of rapamycin on longevity and glucose homeostasis can be uncoupled.

Our results suggest that rapamycin extends life span, at least in part, by inhibition of mTORC1 and despite impairing glucose homeostasis by means of disruption of mTORC2 signaling. Female *mtor*$^{+/-}$ *mlst8*$^{+/-}$ mice, which had selectively impaired mTORC1 signaling, had increased longevity without overt changes in insulin signaling. Our findings emphasize that mTORC2 disruption profoundly affects metabolism and may be relevant to the pathogenesis of type 2 diabetes and the metabolic syndrome. *S6K1*$^{-/-}$ mice, which, like *mtor*$^{+/-}$ *mlst8*$^{+/-}$ mice, exhibit female-specific life-span extension, are resistant to diet-induced weight gain and insulin resistance (*8*). However,

mtor$^{+/-}$ *mlst8*$^{+/-}$ mice did not display these phenotypes (fig. S12), which demonstrated that factors related to energy balance can also be uncoupled from longevity. Specific disruption of mTORC2 extends life span in worms fed a nutrient-rich diet (*30*). If this effect is conserved in mammals, disruption of mTORC2 may contribute to the prolongevity effect of rapamycin. Nevertheless, our present findings suggest that specific inhibitors of mTORC1 might provide many of the benefits of rapamycin on health and longevity, while avoiding side effects that currently limit its utility.

References and Notes

1. S. J. Olshansky, *Am. J. Public Health* **75**, 754 (1985).
2. D. E. Harrison *et al.*, *Nature* **460**, 392 (2009).
3. C. Chen, Y. Liu, Y. Liu, P. Zheng, *Sci. Signal.* **2**, ra75 (2009).
4. M. Kaeberlein *et al.*, *Science* **310**, 1193 (2005).
5. P. Kapahi *et al.*, *Curr. Biol.* **14**, 885 (2004).
6. O. Medvedik, D. W. Lamming, K. D. Kim, D. A. Sinclair, *PLoS Biol.* **5**, e261 (2007).
7. T. Vellai *et al.*, *Nature* **426**, 620 (2003).
8. C. Selman *et al.*, *Science* **326**, 140 (2009).
9. R. J. Colman *et al.*, *Science* **325**, 201 (2009).
10. R. Weindruch, R. L. Walford, *The Retardation of Aging and Disease by Dietary Restriction* (C.C. Thomas, Springfield, IL, 1988).
11. I. Bjedov *et al.*, *Cell Metab.* **11**, 35 (2010).
12. L. Bordone, L. Guarente, *Nat. Rev. Mol. Cell Biol.* **6**, 298 (2005).
13. H. Y. Lee *et al.*, *Cell Metab.* **12**, 668 (2010).
14. F. P. Dominici, S. Hauck, D. P. Argentino, A. Bartke, D. Turyn, *J. Endocrinol.* **173**, 81 (2002).
15. M. Blüher, B. B. Kahn, C. R. Kahn, *Science* **299**, 572 (2003).
16. R. M. Anson *et al.*, *Proc. Natl. Acad. Sci. U.S.A.* **100**, 6216 (2003).
17. C. Selman *et al.*, *FASEB J.* **22**, 807 (2008).
18. A. Taguchi, L. M. Wartschow, M. F. White, *Science* **317**, 369 (2007).
19. Y. Zheng *et al.*, *J. Endocrinol.* **203**, 337 (2009).
20. J. T. Cunningham *et al.*, *Nature* **450**, 736 (2007).
21. M. Fraenkel *et al.*, *Diabetes* **57**, 945 (2008).
22. V. P. Houde *et al.*, *Diabetes* **59**, 1338 (2010).
23. O. Johnston, C. L. Rose, A. C. Webster, J. S. Gill, *J. Am. Soc. Nephrol.* **19**, 1411 (2008).
24. A. Teutonico, P. F. Schena, S. Di Paolo, *J. Am. Soc. Nephrol.* **16**, 3128 (2005).
25. D. D. Sarbassov *et al.*, *Mol. Cell* **22**, 159 (2006).
26. J. M. García-Martínez, D. R. Alessi, *Biochem. J.* **416**, 375 (2008).
27. C. F. Bentzinger *et al.*, *Cell Metab.* **8**, 411 (2008).
28. N. Cybulski, P. Polak, J. Auwerx, M. A. Rüegg, M. N. Hall, *Proc. Natl. Acad. Sci. U.S.A.* **106**, 9902 (2009).
29. A. Kumar *et al.*, *Diabetes* **59**, 1397 (2010).
30. A. A. Soukas, E. A. Kane, C. E. Carr, J. A. Melo, G. Ruvkun, *Genes Dev.* **23**, 496 (2009).

Acknowledgments: We thank all the members of the Baur and Sabatini laboratories, especially D. Frederick, A. Hutchins, P. Hsu, H. Keys, N. Kalaany, M. Laplante, M. Pacold, and Y. Sancak for help with protocols, reagents, and advice. We also thank D. Cohen and D. Harrison for valuable advice and consultation, C. Patterson for critical reading of the manuscript, and G. Bell of the Whitehead Institute Bioinformatics and Research Computing group for help with statistical analysis and R. The *mtor*-, *Raptor*-, and *mlst8*-deficient mice were generated in collaboration with Bristol-Meyers Squibb. *Rictor* conditional knockout mice were the kind gift of M. Magnuson. This project was supported by a research grant from the American Federation for Aging Research (AFAR) and a Bingham Trust Pilot Award from Penn's Institute on Aging to J.A.B.; a grant from NIH (CA129105) and awards from AFAR, the Starr Foundation, the Koch Institute Frontier Research Program, and the Ellison Medical Foundation to D.M.S.; and a Damon Runyon Fellowship to D.A.G. D.W.L. was supported by a Ruth L. Kirschstein National Research Service Award (1F32AG032833-01A1), L.Y. is supported by a postdoctoral fellowship from the American Heart Association (7600031), and P.K. is supported by the Academy of Finland and the Foundations' post-doc pool. Core services were provided by Penn's Diabetes and Endocrinology Research Center (P30DK19525). D.M.S. is an investigator of the Howard Hughes Medical Institute.

Supporting Online Material

www.sciencemag.org/cgi/content/full/335/6076/1638/DC1
Materials and Methods
Figs. S1 to S12
Table S1
References (*31*–*41*)

11 October 2011; accepted 7 February 2012
10.1126/science.1215135

hnRNP C Tetramer Measures RNA Length to Classify RNA Polymerase II Transcripts for Export

Asako McCloskey,[1] Ichiro Taniguchi,[1] Kaori Shinmyozu,[2] Mutsuhito Ohno[1]*

Specific RNA recognition is usually achieved by specific RNA sequences and/or structures. However, we show here a mechanism by which RNA polymerase II (Pol II) transcripts are classified according to their length. The heterotetramer of the heterogeneous nuclear ribonucleoprotein (hnRNP) C1/C2 measures the length of the transcripts like a molecular ruler, by selectively binding to the unstructured RNA regions longer than 200 to 300 nucleotides. Thus, the tetramer sorts the transcripts into two RNA categories, to be exported as either messenger RNA or uridine-rich small nuclear RNA (U snRNA), depending on whether or not they are longer than the threshold, respectively. Our findings reveal a new function of the C tetramer and highlight the biological importance of RNA recognition by the length.

Different RNA species are exported from the nucleus in distinct complexes (*1*), whose protein compositions can regulate downstream gene expression (*2*, *3*). Among them, spliceosomal U small nuclear RNA (snRNA) and mRNA precursors are similarly transcribed by polymerase II (Pol II) and therefore initially acquire m^{7}G-cap structures, to which the common factor, cap-binding complex (CBC), binds (*1*). However, their export complex assemblies are subsequently different. In U snRNA export, an adaptor protein PHAX binds to both CBC and RNA near the cap, and PHAX subsequently recruits CRM1-RanGTP (*4*). In contrast, in bulk mRNA export, RNA-binding adaptor proteins, such as Aly/REF, are first recruited to the RNA, often in the context of larger protein complexes, the transcription/export (TREX) complex, and/or the exon junction complex (EJC). These adaptor proteins subsequently recruit the major mRNA export receptor TAP/NXF1 to the RNA (*1*, *5*). The mRNA export complex normally lacks U snRNA export factors, such as PHAX (*6*, *7*). Thus, these two RNAs, although they share some similarities, must have distinguishing features that are recognized by the cellular RNA export machinery. One of them is related to the RNA length (*6*–*8*). m^{7}G-capped transcripts take either the U snRNA or mRNA export pathway, depending on their lengths rather than on their sequences. The threshold length for this phenomenon is around 200 to 300 nucleotides (nt), except for highly structured RNA regions, which are incompetent for exerting this RNA length effect (*6*–*8*). We developed an in vitro system that recapitulates the remodeling of RNA-protein complexes according to RNA length to address this issue. In vitro transcribed RNAs of various lengths were mixed with recombinant CBC and glutathione S-transferase (GST)–PHAX fusion protein, and a GST pull-down assay was used to examine the formation of the trimeric complex of RNA, CBC, and PHAX (Fig. 1A). PHAX associated with all the m^{7}G-capped RNAs regardless of their length, indicating that the in vivo situation was not recapitulated in this purified system (Fig. 1A, lane 4). In contrast, when an aliquot of a HeLa nuclear extract (HNE) was added to the system, PHAX binding to the longer RNAs was specifically inhibited (Fig. 1A, lanes 5 to 8). This activity did not require adenosine triphosphate hydrolysis (fig. S1). PHAX binding to some RNAs, like U1 and A-capped U1+50, was stimulated by HNE. This activity was distinct from the inhibitory activity on PHAX recruitment and will be discussed elsewhere.

This inhibitory activity on PHAX recruitment was biochemically purified from HNE [see supporting online material (SOM)]. The final purified fractions contained two major proteins whose appearance correlated with the activity (Fig. 1B and fig. S2). Mass spectrometric analyses revealed that these proteins corresponded to hnRNP C1 and C2 proteins. hnRNP C1 and C2 are nuclear RNA-binding proteins that form a 3:1 heterotetramer

[1]Institute for Virus Research, Kyoto University, Kyoto 606-8507, Japan [2]RIKEN Center for Developmental Biology, Kobe, Hyogo 650-0047, Japan

*To whom correspondence should be addressed. E-mail: hitoohno@virus.kyoto-u.ac.jp